

Compact Tb doped fiber optic current sensor with high sensitivity

Duanni Huang,* Sudharsanan Srinivasan, and John E. Bowers

Electrical and Computer Engineering Department, University of California Santa Barbara, California 93106, USA

*duanni@umail.ucsb.edu

Abstract: A highly sensitive fiber optic current sensor using terbium doped fiber is presented. The Verdet constant of the terbium doped fiber at 1300nm is found to be 19.5 μ rad/A using both a polarimetric and interferometric type sensor. Measurements on a Sagnac-loop sensor using 10cm of terbium doped fiber placed inside a solenoid show over 40dB of open loop dynamic range as well as a minimum detectable current of 0.1mA. Extrapolations of our measurements show that in a practical setup with Tb fiber wrapped around a current carrying wire, the optimal configuration is a 0.5m piece of Tb fiber with a noise limit of 22mA/ $\sqrt{\text{Hz}}$. This sensor is promising for current sensing applications that require high sensitivity and small size, weight, and power.

©2015 Optical Society of America

OCIS codes: (060.2370) Fiber optics sensors; (230.2240) Faraday effect.

References and links

1. R. M. Silva, H. Martins, I. Nascimento, J. M. Baptista, A. L. Ribeiro, J. L. Santos, P. Jorge, and O. Frazão, "Optical current sensors for high power systems: a review," *Appl. Sci.* **2**(4), 602–628 (2012).
2. K. Bohnert, P. Gabus, H. Brändle, and P. Guggenbach, "Fiber-optic dc current sensor for the electro-winning industry," *Proc. SPIE* **5855**, 210–213 (2005).
3. J. Noda, T. Hosaka, Y. Sasaki, and R. Ulrich, "Dispersion of Verdet constant in stress-birefringent silica fibre," *Electron. Lett.* **20**(22), 906–908 (1984).
4. D. Tang, A. H. Rose, G. W. Day, and S. M. Etzel, "Annealing of linear birefringence in single-mode fiber coils: application to optical fiber current sensors," *J. Lightwave Technol.* **9**(8), 1031–1037 (1991).
5. R. Ulrich and A. Simon, "Polarization optics of twisted single-mode fibers," *Appl. Opt.* **18**(13), 2241–2251 (1979).
6. A. H. Rose, Z. B. Ren, and G. W. Day, "Twisting and annealing optical fiber for current sensors," *J. Lightwave Technol.* **14**(11), 2492–2498 (1996).
7. N. Peng, Y. Huang, S. Wang, T. Wen, W. Liu, Q. Zuo, and L. Wang, "Fiber optic current sensor based on special spun highly birefringent fiber," *IEEE Photonics Technol. Lett.* **25**(17), 1668–1671 (2013).
8. R. Laming and D. N. Payne, "Electric current sensors employing spun highly birefringent optical fibers," *J. Lightwave Technol.* **7**(12), 2084–2094 (1989).
9. J. Ballato and E. Snitzer, "Fabrication of fibers with high rare-earth concentrations for Faraday isolator applications," *Appl. Opt.* **34**(30), 6848–6854 (1995).
10. L. Sun, S. Jiang, and J. R. Marciano, "Compact all-fiber optical Faraday components using 65-wt%-terbium-doped fiber with a record Verdet constant of -32 rad/(Tm)," *Opt. Express* **18**(12), 12191–12196 (2010).
11. L. Sun, S. Jiang, and J. R. Marciano, "All-fiber optical magnetic-field sensor based on Faraday rotation in highly terbium-doped fiber," *Opt. Express* **18**(6), 5407–5412 (2010).
12. M. J. Heck, J. F. Bauters, M. L. Davenport, J. K. Doylend, S. Jain, G. Kurczveil, S. Srinivasan, Y. Tang, and J. E. Bowers, "Hybrid silicon photonic integrated circuit technology," *IEEE J. Sel. Top. Quantum Electron.* **19**(4), 6100117 (2013).
13. S. Srinivasan, R. Moreira, D. Blumenthal, and J. E. Bowers, "Design of integrated hybrid silicon waveguide optical gyroscope," *Opt. Express* **22**(21), 24988–24993 (2014).
14. S. Srinivasan and J. E. Bowers, "Integrated high sensitivity hybrid silicon magnetometer," *IEEE Photonics Technol. Lett.* **26**(13), 1321–1324 (2014).
15. H. C. Lefevre, *The Fiber-Optic Gyroscope* (Artech House, 1993).
16. K. Bohnert, P. Gabus, J. Nehring, and H. Brandle, "Temperature and vibration insensitive fiber-optic current sensor," *J. Lightwave Technol.* **20**(2), 267–276 (2002).
17. P. A. Nicati and P. Robert, "Stabilised current sensor using Sagnac interferometer," *J. Phys. E Sci. Instrum.* **21**(8), 791–796 (1988).

18. C. J. Kay, "Serrrodyne modulator in a fibre-optic gyroscope," in *IEE Proceedings J. Optoelectronics* (IET, 1985) pp. 259–264.
 19. G. Frosio and R. Dändliker, "Reciprocal reflection interferometer for a fiber-optic Faraday current sensor," *Appl. Opt.* **33**(25), 6111–6122 (1994).
-

1. Introduction

Fiber optic current sensors (FOCS) based on the Faraday effect have been a topic of interest to the scientific community for over 30 years. Compared with conventional current sensors, FOCS offer several advantages [1]. They are resistant to electromagnetic interference due to their optical operating principle, and offer high common-mode rejection of spurious signals due to the tight control of the optical path. For example, an FOCS wrapped around a current carrying wire will be insensitive to almost all nearby electromagnetic fields except the ones produced by the wire. Furthermore, fiber optic sensors have wide dynamic range, and are able to sense currents up to hundreds of kilo amperes (kA) with negligible saturation effects [2]. Finally, the electronics accompanying the OCS can be easily isolated from the high potentials of the sensing area. However, it is well documented that one drawback of fiber OCS is the presence of linear birefringence within the sensing fiber, which considerably dampens the measured signal, reducing the sensitivity of the sensor. This problem is compounded by the low Verdet constant of standard silica fibers (1 $\mu\text{rad}/\text{A}$ at 1300nm) [3], which means the sensing fiber is often tens or hundreds of meters long and suffer from bend and stress induced birefringence. This led to the development of thermally annealed fibers and twisted fibers, which reduced or suppressed the linear birefringence at the cost of weaker mechanical strength [4–6]. Spun highly birefringent fiber has also been demonstrated to be a promising candidate for FOCS [7,8].

An alternate approach to achieving high sensitivity FOCS is to increase the Verdet constant of the sensing fiber through doping with rare earth materials [9]. A higher Verdet constant decreases the length of fiber needed for high sensitivity, leading to compact, high sensitivity FOCS. Doping the fiber core with terbium (Tb) has been shown to be an effective way of increasing Verdet constant, up to a reported 40 $\mu\text{rad}/\text{A}$ at 1064nm [10], and was utilized in a magnetic field sensor using polarimetric detection [11]. In this work, we utilize a similar 10 centimeter long piece of Tb doped fiber provided by Advalue Photonics to construct a polarimetric as well as a Sagnac-loop based interferometric FOCS. The two sensor measurements of the Verdet constant show excellent agreement at 19.5 $\mu\text{rad}/\text{A}$, or equivalently 15.5 $\text{rad}/\text{T}/\text{m}$ at 1300nm. We verify that this high Verdet constant leads to high sensitivity for the Sagnac-loop FOCS, and extrapolate our results to longer Tb fibers for practical applications.

2. Direct detection (polarimetric)

Direct detection measures the polarization rotation of linearly polarized light as it passes through the sensing fiber. The amount of polarization rotation is given by the Faraday rotation, or $\theta_f = VNI$ where θ_f is the Faraday rotation, V is the Verdet constant, N is the number of solenoid turns around the Tb fiber, and I is the applied current. Since the Tb fiber (10cm) is shorter than the length of the 710 turn solenoid (14cm), we calculate $N = 507$, assuming uniform turn density within the solenoid. A short length of SMF and PM fiber (2cm each) is also in overlap with the solenoid, but we neglect their contributions to Faraday rotation since their Verdet constant is much lower and the overlap is small. For 1A of DC current through the solenoid, we measure 6.5mT of B-field through an independent gaussmeter measurement. The detection scheme is depicted below in Fig. 1.

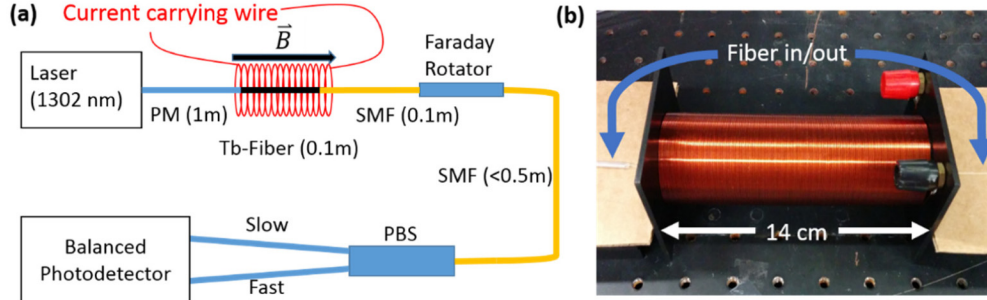


Fig. 1. (a) Schematic of the polarization detection scheme. The sensor consists of a laser, the Tb fiber chain, a Faraday rotator, an in-line polarization beam splitter (PBS), as well as a balanced photodetector. (b) Picture of the 14cm long, 710 turn solenoid coil used to produce the magnetic field.

It is desirable to operate the sensor within telecom O (1260-1360nm) or C (1530-1565nm) bands due to wide availability of light sources and other optical components. Furthermore, rapid advancements in silicon photonics have shown that it is possible to fabricate photonic integrated circuits with high levels of complexity and performance [12]. Thus, the size and cost of optical sensors can be greatly decreased through integration of laser sources and modulators, as proposed in [13,14]. At 1300nm, the total loss of the Tb fiber chain is measured to be 2.3dB. After subtracting 1.5dB of estimated loss from the two splices due to mode mismatch between the Tb fiber and PM or SMF (measured by Advalue Photonics at 1060nm), we obtain a propagation loss of 0.08 dB/cm at 1300nm. At 1550nm, the loss is considerably higher at 1.7dB/cm, and the Verdet constant is expected to be smaller at longer wavelengths [3]. For these reasons, a 1300nm semiconductor laser with 10 dBm output power is used as the source.

The light propagates through the Tb fiber chain, and through an in-line Faraday rotator that provides 45 degrees of polarization shift. Finally, the light passes through an in-line polarization beam splitter, and the intensity difference between the fast and slow axes is measured with a balanced detector. The total length of SMF in the sensor is kept short to minimize sensor size as well as polarization drift.

The intensities of each arm at the detector can be expressed as $P_{slow} = P_0 \cos^2(\theta + \theta_f)$ and $P_{fast} = P_0 \sin^2(\theta + \theta_f)$ where P_0 is the incident light power at the PBS and θ is the 45 degree polarization shift from the Faraday rotator. The normalized signal at the detector can be written as the following, for small Faraday rotation.

$$P_{BD} = \frac{P_0 \cos^2(\theta + \theta_f) - P_0 \sin^2(\theta + \theta_f)}{P_0 \cos^2(\theta + \theta_f) + P_0 \sin^2(\theta + \theta_f)} = \cos(2(\theta + \theta_f)). \quad (1)$$

$$P_{BD} = \cos(2\theta) \cos(2\theta_f) - \sin(2\theta) \sin(2\theta_f) \approx -(2\theta_f) \quad (2)$$

Thus, we expect a linear relation between the power at the detector and the applied current. Furthermore, the slope of the data is $-2VN$, and the Verdet constant of the fiber at 1300nm can be extracted. The figure below shows the detected powers as the DC current through the solenoid is swept from -1A to 1A and back over five minutes.

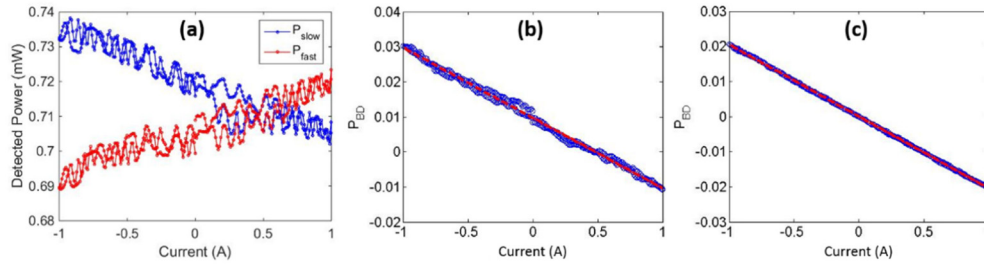


Fig. 2. (a) Individual powers received at the detector from the two orthogonal polarizations. (b) Balanced detection cancels out any fluctuations in power. (c) The current sensor can be improved further by tracking the exact polarization shift in the absence of magnetic field.

From Fig. 2, we can clearly see the benefits of balanced detection. The source power fluctuation is $<1.5\%$, but still creates ripples as shown in Fig. 2(a), but not present in Fig. 2(b). A further improvement can be made by tracking the polarization of light without the applied Faraday rotation during the sweep as seen in Fig. 2(c), which corrects for the polarization drift away from $\theta = 45^\circ$ provided by the Faraday rotator. Here, a “zero-current” point was measured during the current sweep every 10 seconds over the five minute duration of the sweep. From this data, the calculated Verdet constant of the Tb-fiber at 1300nm is $19.5 \mu\text{rad/A}$. This is lower than the previously reported $40 \mu\text{rad/A}$ at 1060nm, but the lower value is expected due to the wavelength dependence of the Verdet constant. The standard deviation from the linear fit is 27mA without polarization tracking in Fig. 2(b), and 5mA with the polarization tracking in Fig. 2(c).

While the simplicity of polarimetric current detection is attractive and the Verdet constant can be easily extracted from the data, it suffers from long term drift. Even over a short 5 minute span as shown in Fig. 2(b), there is evidence of drift in the system in the absence of any feedback. For this reason, it is generally favorable to use interferometric detection schemes.

3. Sagnac-based detection (interferometric)

The second method, as depicted below in Fig. 3, uses a Sagnac loop interferometer which measures the interference between two counter-propagating paths of light through the Tb fiber. The Sagnac loop architecture has been extensively studied and used in high sensitivity fiber optic gyroscopes [15] as well as FOCS [16,17]. The primary difference in the Sagnac configuration for FOCS and gyroscope is the requirement of circular polarization for light within the loop in order to induce a nonreciprocal phase shift.

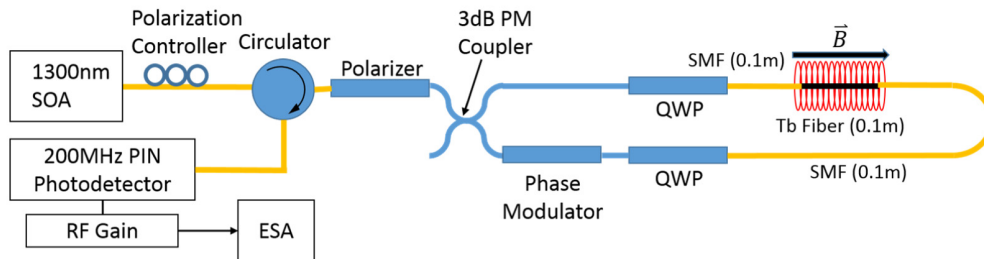


Fig. 3. Schematic of the Sagnac-loop current sensor.

A semiconductor optical amplifier (SOA) pumps 4mW of amplified spontaneous emission (ASE) centered at 1300nm into the sensor. This is preferable to a laser due to the low optical coherence of the ASE, which reduces noise from backscattering within a coherence length from the center of the Sagnac loop. The measured RIN of this source is -130dB/Hz . The light

is polarized, and split into two paths through the 3dB coupler. Within the Sagnac loop, the linear polarization of light is transformed to circular polarization using quarter wave rotator from Fibercore. The two circularly polarized waves then pass through the Tb fiber chain, where they undergo the nonreciprocal phase shift caused by the applied current. A lithium niobate modulator is used to modulate the phases of the counter-propogating light waves with an amplitude of 1.8 radians. The modulation frequency is 15.1 MHz, as governed by the loop length (6.8m).

The nonreciprocal phase shift can be detected by interference at the 3dB coupler, and measured using a photodetector with subsequent RF gain with a combined responsivity of 5300V/W. The total detected optical power at the photodetector is 80μW. Finally, the signal is analyzed with an electrical spectrum analyzer, and the Faraday signal at the first harmonic of the modulation frequency is shown below.

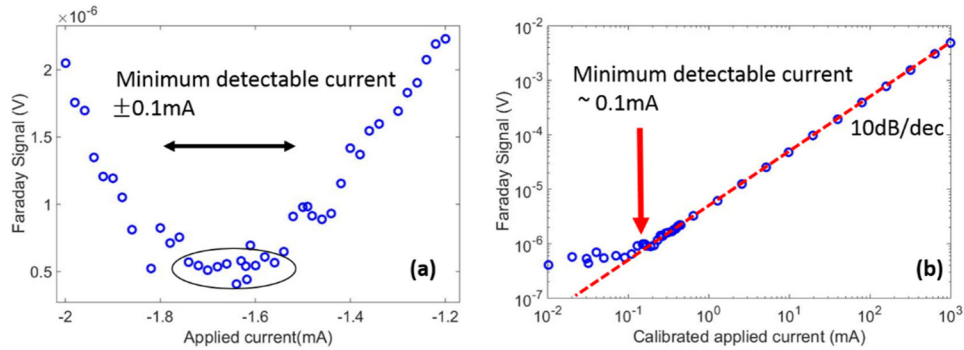


Fig. 4. (a) The Faraday signal after applying RF gain. Measurements show that there is an offset of roughly -1.65mA in the system. (b) The Faraday signal measured over a much wider range of currents, after correcting the -1.65mA offset. Measurements exactly follow the predicted 10dB/dec slope until the applied current is $\sim 0.1\text{mA}$, which is the minimum detectable current for the system.

We sweep the applied current from -1A to 1A , and zoom in on the region of interest where the Faraday signal is at a minimum, as depicted in Fig. 4(a). The minimum of the Faraday signal occurs at -1.65mA . Several causes for this offset are discussed in the next section. Furthermore, there is a 0.1mA window on either side of the minimum point for which there is no change in the Faraday signal, as illustrated by the oval. This suggests that the sensor cannot accurately detect currents in that range. This is better depicted in Fig. 4(b), in which we clearly observe a rolloff in the slope for an applied current below the minimum detectable current of 0.1mA . The dynamic range of the system in this open-loop configuration is over 40dB and can be improved further with feedback techniques or serrodyne modulation [18].

The Verdet constant of the fiber can also be extracted from Fig. 4. Due to the sinusoidal modulation of the phase modulator, the Faraday signal is given by the following.

$$V_{Faraday}(\theta_f) = P_0 \eta J_1(1.8) \sin(2\theta_f) \quad (3)$$

Here, P_0 is the $80\mu\text{W}$ of detected optical power, η is the 5300V/W total responsivity, and $J_1(1.8)$ is the Bessel function of the first order at its maximum modulation amplitude of 1.8 radians. Once again assuming small angle approximation, we calculate the Verdet constant to be $19.3 \mu\text{rad/A}$. This is in excellent agreement with the results from the polarimetric sensor.

4. Analysis and discussion

As previously mentioned, there is a -1.65mA current offset in the Sagnac loop system. We show the measured Faraday signal on the ESA for three different applied currents in Fig. 5(a).

The plot is centered at the 15.1MHz modulation frequency, and the resolution bandwidth is 1Hz.

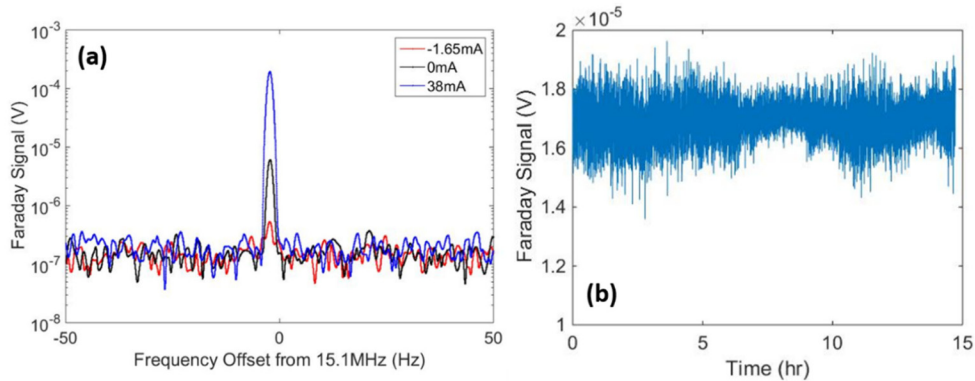


Fig. 5. (a) Measurements of the detected Faraday signal on the ESA for three applied currents. (b) Long term stability plot of the OCS over 15 hours of measured data.

For no applied current in the solenoid, there is a Faraday signal of $6.14\mu\text{V}$, or $12.5\mu\text{rad}$ of Faraday rotation. One possible cause for this is the Earth's magnetic field, which is on the order of $20\text{-}50\mu\text{T}$ in Santa Barbara, which translates to $13\text{-}32\mu\text{rad}$ of Faraday rotation in our system. The solenoid is wrapped in mu-metal for magnetic shielding, but it is difficult to shield all fields due to the experimental configuration in which the sensor is sensitive to fields that run parallel with the fiber. If the fiber was wrapped around a current carrying wire instead, the effects of Earth's magnetic field should be greatly reduced. Another possible cause is amplitude modulation effects in the lithium niobate phase modulator. Nevertheless, these are effects that can be calibrated for, as we have shown.

Another point of interest in Fig. 5(a) is the noise floor of the current sensor. The white noise floor spectral density is roughly $0.20\mu\text{V}/\sqrt{\text{Hz}}$, which corresponds to $0.04\text{mA}/\sqrt{\text{Hz}}$ using the appropriate conversions. However, we are not able to completely reach this white noise floor, as there is residual colored noise in the system. The peak Faraday signal at -1.65mA has a noise spectral density of $0.51\mu\text{V}/\sqrt{\text{Hz}}$, which corresponds to $0.10\text{mA}/\sqrt{\text{Hz}}$. For our resolution bandwidth of 1Hz, this is exactly 0.1mA , and matches the results found in Fig. 4.

Next, we analyze the long term behavior of the sensor in Fig. 5(b). Here, a current of 2mA was applied to the solenoid over 15 hours, and the Faraday signal was recorded every 5 seconds. The standard deviation over all the data points is $0.67\mu\text{V}$, or equivalently 0.14mA . This is very close to the noise limit of the system, and shows that the long term stability is quite good.

Since the Faraday rotation will increase with longer fiber length, we can extrapolate our results for longer Tb fiber. For this extrapolation, we assume a practical setup in which the Tb doped fiber is wrapped around a straight current carrying wire. As the diagram shows in Fig. 6(a), our measured data for a $N = 507$ solenoid can be carried over into an equivalent setup with 507 turns of 10cm circumference fiber. From here, we calculate the sensitivity for a single loop of fiber, and then extrapolate for longer lengths. The limiting factor is the 0.08dB/cm propagation loss of the Tb fiber, which is modelled in Fig. 6(b), assuming the same noise floor for our system.

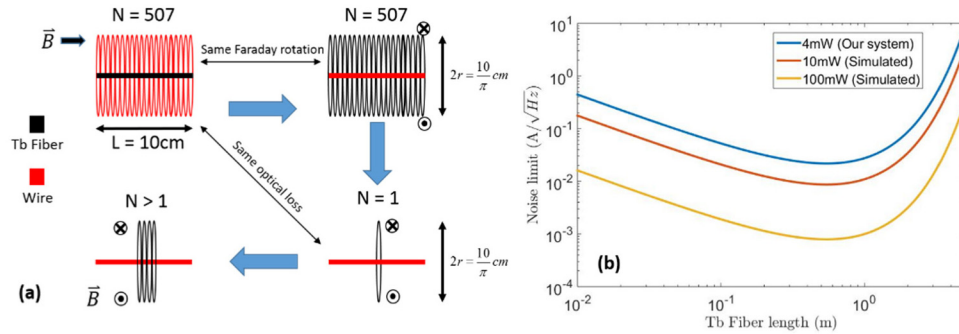


Fig. 6. (a) Conversion from our experimental setup (top left) to a more practical current sensing setup with a straight wire and loops of fiber (top right). To keep the same optical loss, we keep the same length of fiber (bottom right). Now, we can extrapolate the results to multiple loops of fiber (bottom left). (b) Extrapolation of FOCS performance vs length of Tb fiber given our system noise floor and measured propagation loss for various ASE output powers.

The optimal length is for 0.5m of Tb fiber, for which the noise limit is $22\text{mA}/\sqrt{\text{Hz}}$. For even longer fibers, the exponential decrease of received optical power dominates over the linear increase in sensitivity. If the loss in Tb fiber can be reduced or the incident power is increased, then the noise limit can be pushed further down. Finally, an alternate configuration [19] using an in-line reflection based interferometer can demonstrate a higher sensitivity by a factor of two, and will be a topic of exploration in the future.

5. Conclusions

To the best of our knowledge, we have reported the first Sagnac-based FOCS using Tb doped fiber with high Verdet constant of $19.5\mu\text{rad}/\text{A}$ at the operating wavelength of 1300nm. We are able to sense DC currents down to 0.1mA using a test setup with a 507 turn solenoid. Finally, we extrapolate our measurements to find a noise limit of $22\text{mA}/\sqrt{\text{Hz}}$ for a practical Tb fiber current sensor with a length of just 0.5 meter. This sensor shows promise for high sensitivity applications in which it is not possible to use tens or hundreds of meters of fiber. Further improvements to this technology can be made by spinning the Tb fiber and decreasing the propagation loss.

Acknowledgments

The authors would like to thank TE Connectivity for supporting this research, and Advalue Photonics for providing the Tb doped fibers. We also thank Katya Golovchenko, Yichen Shen, Minh Tran, Daryl Spencer, Tin Komljenovic, Paolo Pintus, and Yifei Li, for helpful suggestions.